http://www.joes.org.in

Journal of Earthquake Science and Engineering, vol. 2(1), pp 1-13

Publisher ISES 2015

Investigating the Effect of Spatial Distribution of Seismicity on Probabilistic Seismic Hazard Results

L.R. Pattanur [1] and I.D. Gupta[2]

[1] Central Water and Power Research Station, Pune, India
[2]Department of Earthquake Engineering, IIT Roorkee, Roorkee, India,

Received: 24/04/2014; Accepted: 19/02 /2015

Abstract

In probabilistic seismic hazard assessment, the seismic source zones in a region under study are generally modeled using the area sources and the seismicity is distributed uniformly over the area of each source zone. It is assumed that future earthquakes are equally likely at all locations in the source. However, the tectonic features and the epicentral distribution of past earthquakes may dictate the use of non-uniform spatial distribution of seismicity within each area source. This paper investigates the effect of spatial distribution of seismicity for assessment of seismic hazards with illustrative examples from the SONATA tectonic province in Central India.

Keywords: Area source, Line source, SONATA zone, Probabilistic seismic hazard, Spatial distribution

1. Introduction

Area types of seismic sources with uniform spatial distribution of seismicity are used commonly in probabilistic seismic hazard assessment for regions where past seismic activity does not correlate with the known tectonic and geological features (Gupta, 2006; 2013; Mandal et al., 2013). However, it may generally be possible to identify portions with relatively higher epicentral density to consider a more realistic non-uniform distribution of the expected seismicity in area sources also. In this paper, it is proposed to assess the seismic hazard by probabilistic approach for the Son-Narmada-Tapti (SONATA) zone in central India by using different plausible spatial distributions for expected future seismicity.

*Corresponding Author
Email: lrpattanur@yahoo.co.in, (L.R. Pattanur)

The SONATA rift zone is an ENE-WSW trending zone and runs across the Indian shield from west coast to east coast and is the most striking feature in the tectonic map of India (Dasgupta et al., 2000). This rift zone of about 1600 km in length separating the northern and southern blocks of the Indian shield is a region of moderate seismic activity with infrequent earthquakes. Due to uniqueness of the geological, structural and seismotectonic features, a number of investigators (e.g.; Choubey, 1971; Yedekar et al., 1990; Rajurkar et al., 1990; Jain et al., 1995; Nair et al., 1995; Mishra and Gupta, 1997; etc.) had chosen this region for detailed investigations in the past.

The most prominent trend in the region is the ENE-WSW Satpura trend of the Central Indian Tectonic Zone (CITZ). The northern and southern extremities of the CITZ are delineated by ENE-WSW trending Son Narmada North Fault (SNNF). The Son Narmada South fault(SNSF). There are several other sub-parallel faults and lineaments in the SONATA zone (Jain et al., 1995).

2. Regional Seismotectonics

The region considered in the present study is bound by latitudes 19°N to 26°N and longitudes 73°E to 82°E. Major seismotectonic features in the region considered are shown in fig. 1 (Dasgupta et al., 2000).

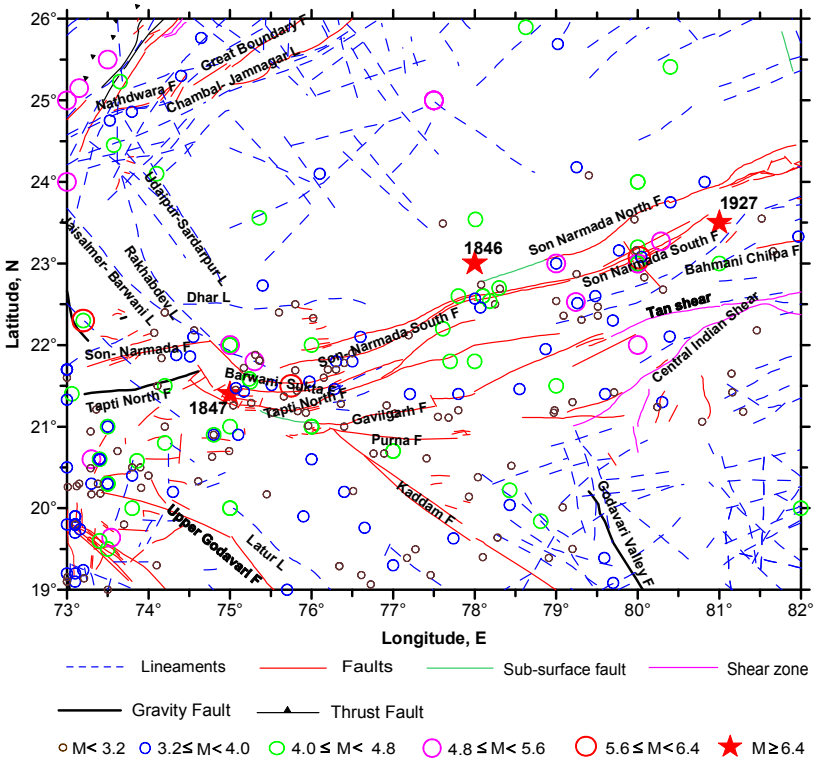

Figure 1. Correlation of past earthquakes with the tectonic features in the study region

The Son-Narmada fault is the longest feature in the region, which does not reveal any major movement in the Deccan Trap in the west, but its easterly stretch is marked by dislocations in the Archaean crystallines, Mahakoshal metasediments and Vindhyan sediments (Mishra and Gupta, 1997; Nair et al., 1995). The SNS fault is another prominent feature, which extends ENE-WSW for about 1,000 km from Khandwa in the west up to Rihand Reservoir and probably beyond in Uttar Pradesh in the east. The active status of this fault is apparent by a sharp contact of the Narmada alluvium with Gondwanas and the Deccan Trap to the south (Rajurkar et al., 1990). Another sympathetic fault runs only a few km (less than 10 km to 40 km) north of the SNS fault.

The Tapti North Fault (TNF), Gavilgarh Fault, Purna Fault, Tan shear are some of the important tectonic features (fig. 1) which have shown neotectonic activity (Shanker, 1987; Yedekar et al., 1990). The Tan shear zone is essentially a ductile shear zone marked by ultramylonite, mylonite and phyllonites. The Purna fault following the course of Purna river displays almost E-W trend in the area. It is traceable for over 200 km from Amravati in the east to Jalgaon in the west, where it merges with the Tapti lineament.

In the southern part of CITZ, the important features are the Upper Godavari fault, the Kaddam Fault and the Godavari Valley Fault (Rajurkar et al., 1990). The Upper Godavari Fault (fig. 1) with WNW-ESE trend traverses the south western portion of the region. The Upper Godavari Fault extends over 280 km from Nasik and can be traced further southeast up to Manjira river where it is termed as the Bir Lineament. Parallel to this fault is the Latur Lineament that passes through north of the epicentral tract of Killari Earthquake of 30 September 1993. The Kaddam Fault trending NW-SE is traceable over a length of 280 km and has been named after the Kaddam River whose course has been controlled by this fault. This fault appears to have been truncated by the Purna lineament of the Satpura trend. Faulting has been recognized in several sectors of this lineament.

3. Identification of Seismic Sources

Possible seismic sources in and around CITZ are identified by analyzing the correlation of past seismicity with the major tectonic features. For this purpose a unified earthquake catalog covering the period from 1702 to 2010 is compiled from various sources. The catalog of India Meteorological Department (IMD) was used as the basic catalog, which was upgraded by adding further data from other important international sources like International Seismological Summary (ISS), International Seismological Center (ISC), National Earthquake Information Center (NEIC) of United States Geological Survey (USGS), and National Oceanic and Atmospheric Administration (NOAA). The catalog thus compiled 122 earthquakes in the magnitude range 3.6 to 6.5.

Fig. 1 also includes epicenters of these past earthquakes along with various tectonic features. As shown in fig. 1 the epicenters broadly follow the trends of major tectonic features, indicating their active status. Considering the spatial distribution and correlation of seismic activity with the tectonic features in the region, following five seismic sources and two sub sources are identified (fig. 2):

Source-1: Son-Narmada-Tapti (SONATA) zone of the Satpura trend

Source-2: Area of Delhi-Aravalli trends

Source-3: Area of Great Boundary Fault

Source-4: Area of Dharwar trend

Source-5: Upper Godavari and West Coast zone

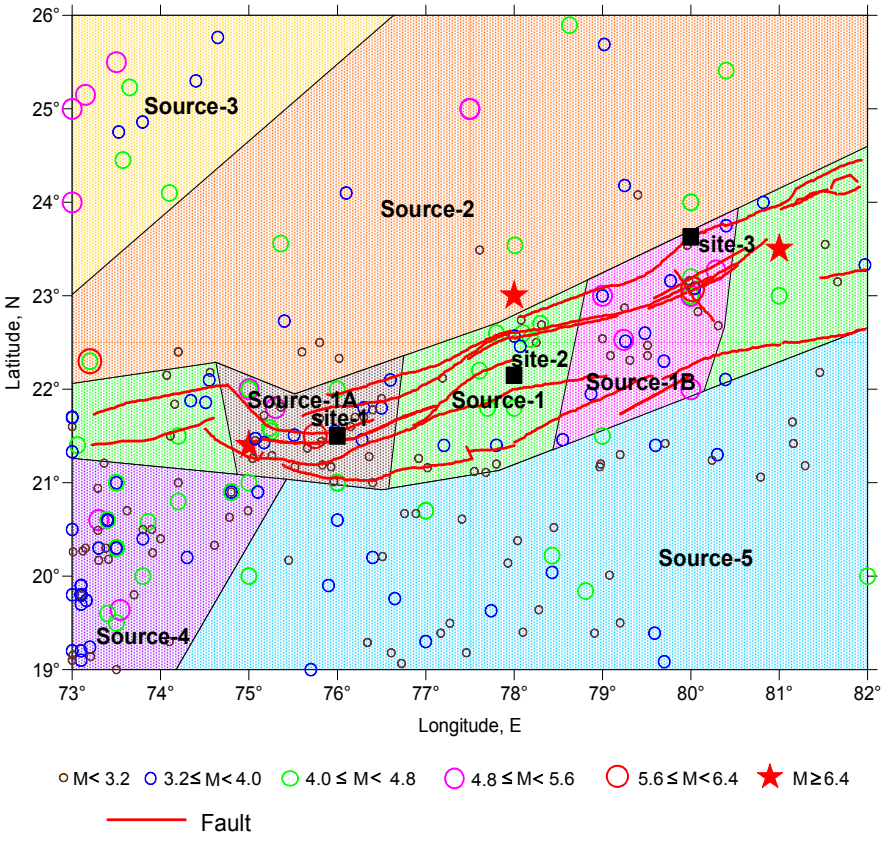

Figure 2. Possible seismic sources identified in the example region along with the epicenters of past earthquakes.

Two sub sources 1A and 1B have been delineated in Source-1 to account for the spatial clustering of epicenters of past earthquakes.

4. Probabilistic Seismic Hazard Analysis

The probabilistic seismic hazard analysis (PSHA) approach considers the effect of total expected seismicity with suitable spatial distribution to evaluate the ground motion amplitudes (e.g., response spectral amplitudes at different periods) at a site with a desired confidence level during a specified exposure period. This approach is based on the following form of composite probability distribution of the spectral amplitude $SA(T)$ at a particular natural period T (McGuire, 1977; Anderson and Trifunac, 1978; Gupta, 2002).

$$P[SA(T)] = \exp\left\{-Y\sum_{i=1}^{I}\sum_{j=1}^{J} q[SA(T) \mid M_j, R_i]\nu(M_j, R_i)\right\} \quad (1)$$

In this expression, $\nu(M_j, R_i)$ is the annual occurrence rate of earthquakes within small magnitude and distance ranges $(M_j - \delta M_j, M_j + \delta M_j)$ and $(R_i - \delta R_i, R_i + \delta R_i)$ in all the seismic sources and Y is the exposure time considered. The quantity $q[SA(T) \mid M_j, R_i, \delta_{ij}]$ is the probability of exceeding the spectral amplitude $SA(T)$ due to earthquake of magnitude M_j at distance R_i, as estimated by the probability distribution of the residuals around the median estimate from an empirical attenuation relationship.

4.1 Attenuation Relationships Used

From a comparison of four selected attenuation relationships due to Abrahamson and Silva (1997), Lee (1987), Toro et el. (1997) modified by Toro (2002), and Ragukanth and Iyengar (2007) with the mean response spectrum of two horizontal components of the accelerogram recorded during Koyna earthquake of 10 December 1967, the relationship due to Lee is found to be more appropriate for Peninsular India (fig. 3).

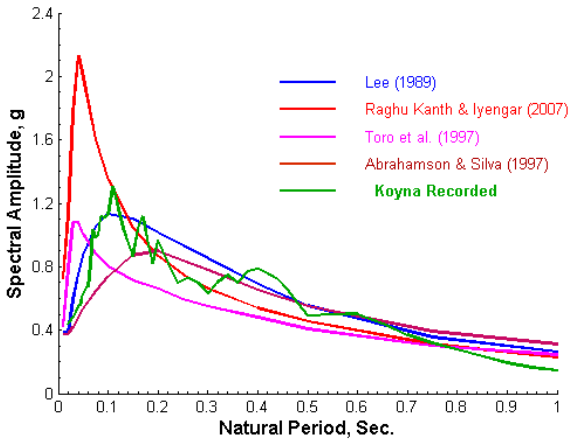

Figure 3. Comparison of four selected attenuation relations with recorded response spectrum for Koyna main earthquake.

Lee (1987) has developed a frequency-dependent attenuation relationship for pseudo spectral velocity (PSV) using a database of about 1500 strong motion accelerograms representing a wide range of recording site conditions, as follows:

$$\log\langle PSV(T)\rangle = M + Att(\Delta, M, T) + b_1(T)M + b_2^{(1)}(T)S^{(1)} + b_2^{(2)}(T)S^{(2)} + b_3(T)v + b_4^{(1)}(T)S^{(1)}v + b_4^{(2)}(T)S^{(2)}v + b_5(T) + b_6(T)M^2 + b_7^{(1)}(T)S_L^{(1)} + b_7^{(2)}(T)S_L^{(2)} \quad (2)$$

In this expression, $\langle PSV(T)\rangle$ represents the least square estimate of *PSV*(*T*) amplitude at natural period *T*, *M* is the earthquake magnitude (M_L up to 6.5 and M_S for higher values), *v* is the component variable (0 for horizontal and 1 for vertical component), and $Att(\Delta, M, T)$ is a period dependent attenuation function defined by Trifunac and Lee (1990) in terms of a representative source to site distance, Δ, which is defined in terms of the epicentral distance, focal depth and the earthquake magnitude. Parameters $S^{(1)}$ and $S^{(2)}$ in eqn. (2) are the indicator variables used to define the site geological condition, which takes the following values

$$S^{(1)} = \begin{cases} 1; \text{ for intermediate type geology} \\ 0; \text{ otherwise} \end{cases}; \quad S^{(2)} = \begin{cases} 1; \text{ for basement rock} \\ 0; \text{ otherwise} \end{cases} \quad (3)$$

Further, parameters $S_L^{(1)}$ and $S_L^{(2)}$ are the indicator variables for the site soil condition, and they take the following values:

$$S_L^{(1)} = \begin{cases} 1; \text{ for stiff soil site} \\ 0; \text{ otherwise} \end{cases}; \quad S_L^{(2)} = \begin{cases} 1; \text{ for deep soil site} \\ 0; \text{ otherwise} \end{cases} \quad (4)$$

Coefficients $b_1(T)$, $b_2(T)$, etc. in eqn. (2) have been obtained by Lee (1987) from a regression analysis of the recorded strong motion data. Lee has also studied the scattering of the observed spectral amplitudes about the mean amplitudes, and showed that the residuals $\varepsilon(T) = \log PSV(T) - \log\langle PSV(T)\rangle$ can be approximated by the following probability distribution function

$$P(\varepsilon) = [1 - \exp(-\exp(\alpha(T)\varepsilon(T) + \beta(T)))]^{N(T)} \quad (5)$$

Parameters $\alpha(T)$, $\beta(T)$ and *N(T)* in this relation have been also obtained by Lee (1987) at different periods by performing a regression analysis of the observed residuals $\varepsilon(T)$. For the probabilistic hazard computation using the expression of eqn. (1) one needs to estimate

the probability $q[PSV(T) \mid M_j, R_i]$ for all expected magnitude and distance pairs (M_j, R_i) in all the seismic sources. This can easily be obtained as the complementary of the probability of eqn. (5) for the residual between a specified value of *PSV*(*T*) and the least square estimate for M_j and R_i,

$$q[PSV(T) \mid M_j, R_i] = 1 - P[\varepsilon(T)] \tag{6}$$

The pseudo velocity spectral amplitudes *PSV*(*T*) in the foregoing description can equivalently be converted in to pseudo acceleration spectral amplitudes *PSA*(*T*) using the following identity:

$$PSA(T) = \left(\frac{2\pi}{T}\right) PSV(T) \tag{7}$$

4.2 Estimation of Design Seismicity

Next, to obtain the seismicity rates $\nu(M_j, R_i)$ required for hazard computation, following form of Gutenberg-Richter's (1944) recurrence relationship is first defined using past earthquake data for each seismic source

$$\log N(M) = a - bM \tag{8}$$

In this expression, *N(M)* is the annual number of earthquakes with magnitude *M* or greater and *a* and *b* are the constants specific to the seismic source of interest.

Table-1. Recurrence parameters and maximum magnitudes considered for various seismic sources.

Sources	b-value	a-value	Mmax
1	0.73	2.68	6.7
1A		2.19	
1B		2.29	
Rest of 1		2.14	
2	0.65	2.06	6.7
3	0.80	2.47	5.1
4	1.09	3.71	5.0
5	0.88	2.66	4.6

To evaluate these constants, the observed rates *N(M)* for different magnitude ranges are estimated using past earthquake data in each source zone for the period for which the data are reported completely. The cut-off magnitude of completeness for different years is obtained using the method of Stepp (1973). Other methods in vogue for the purpose are the maximum curvature (Wiemer and Wyss, 2000) and the entire magnitude range (Ogata and Katsura, 1993) methods. The constants *a* and *b* have been then obtained using the maximum likelihood method of Weichert (1980). The parameters *a* and *b* thus obtained for all the five main sources are given in Table-1. Parameter *a* for sub-sources 1a, 1b and rest of the source zone-1 is obtained by keeping the b-value the same as that for the entire source zone-1.

From knowledge of parameters *a* and *b*, the relationship of eqn. (8) is used to obtain the total number $N(M_{\min})$ of earthquakes above a specified threshold magnitude $M_{\min}$, which can produce ground motion of engineering significance. In the present study, this has been taken as 3.8, which represents epicentral value of MMI just exceeding IV. For practical applications, it is also necessary to consider an upper bound magnitude M_{max} for each seismic source. The maximum magnitudes assigned to various source zones are given in the last column of Table-1. With both upper and lower bound magnitudes, the expression for *N(M)* can be written as (Cornell and Vanmarcke, 1969)

$$N(M) = N(M_{\min}) \frac{\exp(-\beta(M - M_{\min})) - \exp(-\beta(M_{\max} - M_{\min}))}{1 - \exp(-\beta(M_{\max} - M_{\min}))} \qquad (9)$$

Parameter β in this relation is related to the *b* value as $b\ln 10$. Relationship of eqn. (9) describes an exponential decay of *N(M)* with increase in *M* up to the maximum magnitude. A typical example of such a recurrence relationship fitted to the available past earthquake data in seismic source zone-2 is shown in fig.4.

From the recurrence relationship for a source zone, the occurrence rate of earthquakes within a small magnitude range $(M_j - \delta M_j,\ M_j + \delta M_j)$ around magnitude M_j can be obtained as

$$n(M_j) = N(M_j - \delta M_j) - N(M_j + \delta M_j) \qquad (10)$$

To obtain the seismicity $\upsilon(M_j, R_i)$, the number *n(Mj)* is required to be distributed suitably over the entire source area. For sources 2 to 5, the seismicity is assumed to be distributed uniformly. However, to investigate the influence of spatial distribution of seismicity on the seismic hazard, the spatial distribution of seismicity for source-1 is considered in three different ways as follows:

- Uniform distribution over two sub sources as well as over the remaining area.

- Uniform distribution for magnitudes below 5.0 and as per spatially averaged past seismicity for larger magnitudes.
- Uniform distribution for magnitudes below 5.0 over the entire source area and uniform distribution along various known faults for larger magnitudes.

For uniform spatial distribution of seismicity, the source area is discretized into area elements of size 0.1° latitude × 0.1° longitude and the total number is distributed equally among all the elements. For non-uniform distribution, the actually observed number of earthquakes in each area element is converted into an equivalent number of M5.0 events and a spatial averaging of such numbers in all the source elements is performed using a Gaussian filter. The total number is then distributed among all the elements in proportion to the spatially averaged equivalent number of observed M5.0 events. The epicenters of all earthquakes in a source element are assumed to be at its center. To consider uniform distribution along a fault, the fault trace is discretized into linear elements of one kilometer length and the number of earthquakes associated with an element is assumed to be concentrated at its midpoint. Finally, the numbers from all the source elements lying within a small distance range $(R_i - \delta R_i, R_i + \delta R_i)$ from a specified site are clubbed together for each magnitude interval $(M_j - \delta M_j, M_j + \delta M_j)$ to get the desired seismicity rates $\upsilon(M_j, R_i)$. For the present study, the magnitude has been discretized into eight magnitude intervals with the central magnitudes *Mj* = 3.8, 4.2, 4.6, 5.0, 5.4, 5.8, 6.2 and 6.6 with $\delta M_j = 0.2$. The focal depth is assumed to increase linearly from 10 km to 20 km with increase in the magnitude from 3.8 to 6.6.

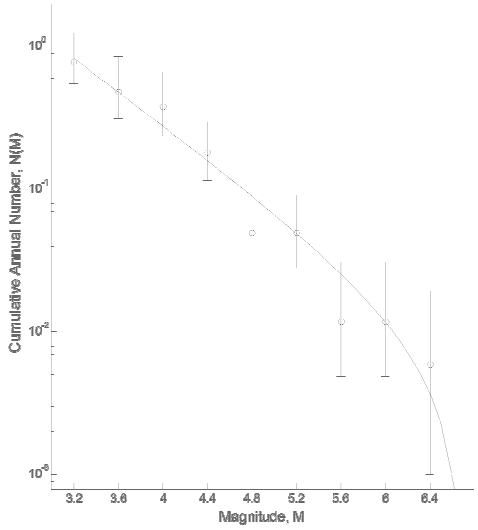

Figure 4. Typical example of the exponentially decaying recurrence relationship

5. Results and Discussion

Spatial distribution of seismicity (seismic sources) is considered to compute the seismic hazard (fig. 2). The seismic hazard is estimated in terms of 5% damped uniform hazard acceleration response spectra of horizontal component on stiff soil site (NEHRP class A) overlying the basement rock. The results for 2% probability of exceeding in 50 years (return period of around 2500 years) are shown in fig. 5. It is seen that different spatial distributions of seismicity have varying effect on the spectral amplitudes at different sites, depending upon the relative concentration of seismicity with respect to the site. Thus it is difficult to know in advance which spatial distribution of seismicity will lead to the most conservative estimate of the hazard. It is thus necessary to consider all plausible spatial distributions by branches of logic tree to consider the epistemic uncertainty in the spatial distribution of expected future seismicity (Gupta, 2005).

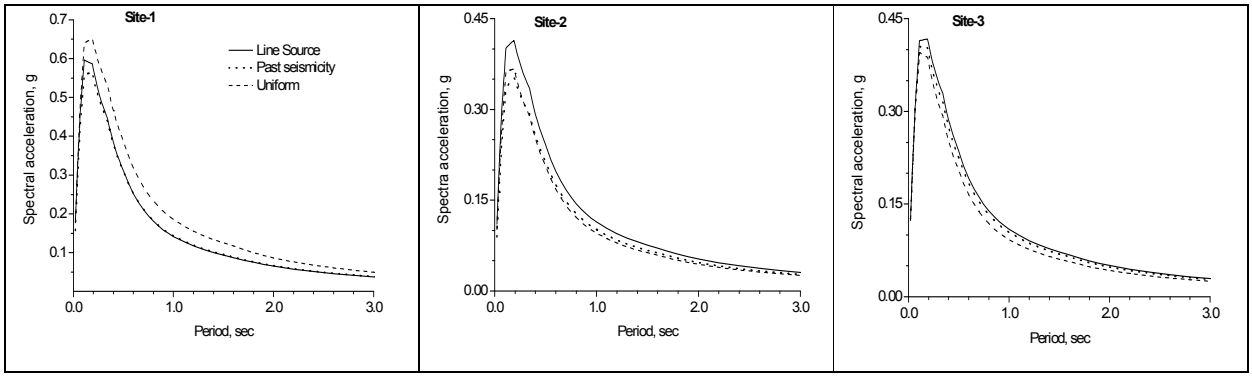

Figure 5. Comparison of the hazard spectra for different spatial distribution of seismicity

A comparison of the results in fig. 5 with the similar results in figure 8b of Mandal et al. (2013) reveals a general compatibility between the two. The differences may be attributed to the spatial distribution of seismicity with respect to the site and the different attenuation relations used. The differences on account of spatial distribution can well be assimilated by the differences for three sites considered in the present study. The differences due to attenuation relation are more prominent and are typical to the nature of the relationships used as can be seen from the comparison in fig. 3. The attenuation relation of Raghukanth and Iyengar used in Mandal et al. (2013) is typical of the attenuation in eastern and central United States with very high amplitude spectral peak at frequencies around 25–30 Hz which decays very fast for lower frequencies. On the other hand, the Koyna spectrum and those of some other records in Peninsular India show quite different behavior with spectral peak around 10–12 Hz and relatively slower decay for lower frequencies. Thus, the present spectra can be considered more realistic for natural periods greater than about 0.3–0.5 s.

References:

Abrahamson, N.A., and W.J. Silva (1997). Empirical response spectral attenuation relations for shallow crustal earthquakes, *Seismological Research Letters,* 68, 94-127.

Anderson, J.G., and M.D. Trifunac (1978). Uniform risk functionals for characterization of strong earthquake ground motion, *Bulletin of Seismological Society of America,* 68(1), 1205-1218.

Cornell, C.A., and E.H. Vanmarcke (1969). The major influence on seismic risk, Procs. 4th World Conf. Earthq. Eng., Santiago, Chile, A-1, 69-93.

Choubey, V.D. (1971). Pre-Deccan Trap topography in Central India and crustal warping in relation to Narmada rift structure and volcanic activity, *Bulletin of Volcanology,* 35, 660-685.

Dasgupta, S., P. Pande, D. Ganguly, Z. Iqbal, K. Sanyal, N.V. Venkataraman, S. Dasgupta, B. Sural, L. Harendranath, K. Mazumdar, S. Sanyal, A. Roy, L.K. Das, P.S. Misra, and H. Gupta (2000). Seismotectonic Atlas of India and its Environs, P.L. Narula, S.K. Acharyya and J. Banerjee (Eds.), *Geological Survey of India* (Special Publication), 59, 87.

Gupta, I.D. (2002). State of the art in seismic hazard analysis, *ISET Journal of Earthquake Engineering,* 39(4), 311-346.

Gupta, I.D. (2005). Probabilistic seismic hazard analysis with uncertainties, *Procs. Symp. Seismic Hazard Analysis & Microzonation,* 23-24 September, IIT Roorkee, Vol. I, 97-117.

Gupta, I.D. (2006). Delineation of probable seismic sources in India and neighbourhood by comprehensive analysis of seismotectonic characteristics of the region, *Soil Dynamics and Earthquake Engineering,* 26, 766-790.

Gupta, I.D. (2013). Source-to-site distance distribution for area type of seismic sources used in PSHA applications, *Natural Hazards,* 66, 485–499.

Gutenberg, B. ,and C.F. Richter (1944). Frequency of earthquakes in California, *Bulletin of Seismological Society of America,* 34(4), 1985-1988.

Jain, S.C., K.K.K. Nair, and D.B. Yedekar (1995). Geology of the Son-Narmada-Tapti lineament zone in Central India, In: Project CRUMANSONATA Geoscientific Studies of

the Son-Narmada-Tapti Lineament Zone, *Geological Survey of India* (Special Publication), 10.

Lee, V.W. (1987). Influence of local soil and geologic site conditions on pseudo relative velocity response spectrum amplitudes of recorded strong motion accelerations, Report CE 87-05, Dept. of Civil Eng., Univ. of Southern California, Los Angeles, California, USA.

Mandal, H.S., A.K. Shukla, P.K. Khan, and O.P. Mishra (2013). A New Insight into Probabilistic Seismic Hazard Analysis for Central India, *Pure and Applied Geophysics,* 170, 2139-2161.

McGuire, R.K. (1977). Seismic design spectra and mapping procedures using hazard analysis based directly on oscillator response, *Earthquake Engineering and Structural Dynamics,* 5, 211-234.

Mishra, D.C., and S.B. Gupta (1997). Structural style of Narmada-Son lineament, *Geological Survey of India* (Miscellaneous Publication), 63, 5-16.

Nair, K.K.K., S.C. Jain, and D.B. Yedekar (1995). Stratigraphy structure and geochemistry of Mahakoshal Greenstone Belt, *Mem. Geol. Soc. India*, 31, 403-432.

Ogata, Y., and K. Katsura (1993). Analysis of temporal and spatial heterogeneity of magnitude frequency distribution inferred from earthquake catalogues, *Geophysical Journal International,* 113, 727-738.

Raghu Kanth, S.T.G., and R N Iyengar (2007). Estimation of seismic spectral acceleration in Peninsular India, *Journal of Earth System Science,* 116(3), 199-214.

Rajurkar, S.T., V.D. Bhate, and S.B. Sharma (1990). Lineament fabric of Madhya Pradesh and Maharashtra and its tectonic significance, *Geological Soc. of India,* (Special Publication), 28, 241-259.

Shanker, R (1987). Neotectonic activity along the Tapti-Satpura lineament in Central India, Ind. Miner, 41, No. 1.

Stepp, J.C. (1973). Analysis of completeness of the earthquake sample in the Puget Sound area, in Seismic Zoning (edited by S.T. Harding), NOAA Tech. Report ERL 267-ESL30, Boulder, Colorado, USA.

Toro, G.R., N.A. Abrahamson, and J.F. Schneider (1997). Model of strong ground motions from earthquakes in central and eastern North America: Best estimates and uncertainties, *Seismological Research Letters,* 68(1), 41-57.

Toro, G.R. (2002). Modification of the Toro et al. (1997) attenuation equations for large magnitudes and short distances, *Risk Engineering, Inc.,* 4-1 to 4-10.

Trifunac, M.D., and V. Lee (1990). Frequency dependent attenuation of strong earthquake ground motion, *Soil Dynamics and Earthquake Engineering,* 9(1), 3-15.

Weichert, D.H. (1980). Estimation of the earthquake recurrence parameters for unequal observation periods for different magnitudes, *Bulletin of Seismological Society of America* ,70(4), 1337-1346.

Wiemer, S., and M. Wyss (2000). Minimum magnitude of complete reporting in earthquake catalogs: examples from Alaska, the western United States, and Japan, *Bulletin of Seismological Society of America,* 90, 859-869.

Yedekar, D.B., S.C. Jain, K.K.K. Nair, and K.K. Dutta (1990). Central India collision suture, Precambrian of Central India, *Geological Survey of India* (Special Publication), 28, 1-45.